

Determining Absorption, Emissivity Reduction, and Local Suppression Coefficients inside Sunspots

Stathis Ilonidis · Junwei Zhao

Received: 13 November 2009 / Accepted: 24 June 2010 / Published online: 28 August 2010

Abstract The power of solar acoustic waves is reduced inside sunspots mainly due to absorption, emissivity reduction, and local suppression. The coefficients of these power-reduction mechanisms can be determined by comparing time-distance cross-covariances obtained from sunspots and from the quiet Sun. By analyzing 47 active regions observed by SOHO/MDI without using signal filters, we have determined the coefficients of surface absorption, deep absorption, emissivity reduction, and local suppression. The dissipation in the quiet Sun is derived as well. All of the cross-covariances are width corrected to offset the effect of dispersion. We find that absorption is the dominant mechanism of the power deficit in sunspots for short travel distances, but gradually drops to zero at travel distances longer than about 6° . The absorption in sunspot interiors is also significant. The emissivity-reduction coefficient ranges from about 0.44 to 1.00 within the umbra and 0.29 to 0.72 in the sunspot, and accounts for only about 21.5% of the umbra's and 16.5% of the sunspot's total power reduction. Local suppression is nearly constant as a function of travel distance with values of 0.80 and 0.665 for umbrae and whole sunspots respectively, and is the major cause of the power deficit at large travel distances.

Keywords: Helioseismology, Sunspots, Absorption, Emissivity reduction, Local suppression, Acoustic waves

1. Introduction

Solar oscillations have lower amplitude in sunspots than in the quiet Sun (Leighton, Noyes, and Simon, 1962; Lites, White, and Packman, 1982). The observed power reduction is caused by several mechanisms which, in this paper, are grouped in three categories: absorption, emissivity reduction, and local suppression, as categorized by Chou *et al.* (2009c).

The first category, absorption, includes three different mechanisms: *i*) acoustic wave energy is converted into heat (Hollweg, 1988; Lou, 1990; Sakurai, Goossens,

W.W. Hansen Experimental Physics Laboratory, Stanford University, Stanford, CA 94305-4085, USA
email: ilonidis@sun.stanford.edu

and Hollweg, 1991; Goossens and Poedts, 1992), *ii*) acoustic waves are converted into modes that cannot be detected in the photosphere (Spruit and Bogdan, 1992; Cally and Bogdan, 1993; Cally, Bogdan, and Zweibel, 1994; Crouch and Cally, 2005; Gordovskyy and Jain, 2008), *iii*) wave leakage to the outer atmosphere is enhanced due to the modification of the acoustic cut-off frequency. The second category is emissivity reduction. The reduction in convection in sunspots leads to reduced excitation of acoustic waves (Hurlburt and Toomre, 1988; Parchevsky and Kosovichev, 2007). The last category, local suppression, is a local change in observed wave amplitude, rather than a change in energy. Several mechanisms also fall into this category. The observed amplitude reduction may be caused by: *i*) Wilson depression (Hindman, Jain, and Zweibel, 1997), *ii*) altered eigenfunctions (Hindman, Jain, and Zweibel, 1997), *iii*) a greater wave speed, and *iv*) a change in the line profile (Wachter, Schou, and Sankarasubramanian, 2006; Rajaguru *et al.*, 2007). For more details on each mechanism see Hindman, Jain, and Zweibel (1997) and Chou *et al.* (2009a, 2009b).

Braun, Duvall, and LaBonte (1987, 1988), Bogdan *et al.* (1993), and Chen, Chou, and the TON team (1996) found, using Hankel analysis and spherical decomposition of the acoustic wavefield, that sunspots absorb as much as 50% of the incoming acoustic waves. This method includes decomposition of the p -mode oscillations into inward and outward propagating modes with respect to the sunspot. However, the effects of absorption and emissivity reduction cannot be distinguished, and, additionally, local suppression is not included in such measurements.

The first attempt to distinguish and determine the three coefficients of absorption, emissivity reduction, and local suppression was made by Chou *et al.* (2009b, 2009c). For this purpose they used the property that the waves emitted along the wave path between two points have no correlation with the signal at the starting point. Their technique makes use of direction and phase-velocity filters, which successfully allow measurements of the three above coefficients for specific acoustic wave-travel distances.

In this work we use a similar yet new method, which does not make use of the direction and phase-velocity filters to determine the coefficients of absorption, emissivity reduction, and local suppression. Instead, we use many active regions to increase the signal-to-noise ratio. The measurement procedure, in the absence of those filters, is more general and does not depend on the particular characteristics of the filters. More specifically, the absence of the phase-velocity filter allows the determination of all three parameters as functions of travel distance from active regions, while the absence of direction filter does not raise any questions regarding the width of the filter. This issue is important in some steps of the measurement procedure such as the correction for the dispersion of acoustic waves. On the other hand, the use of many active regions limits our method to an averaged measurement of absorption, emissivity reduction, and local suppression inside active regions only as functions of travel distance from the center of the regions but not as functions of direction.

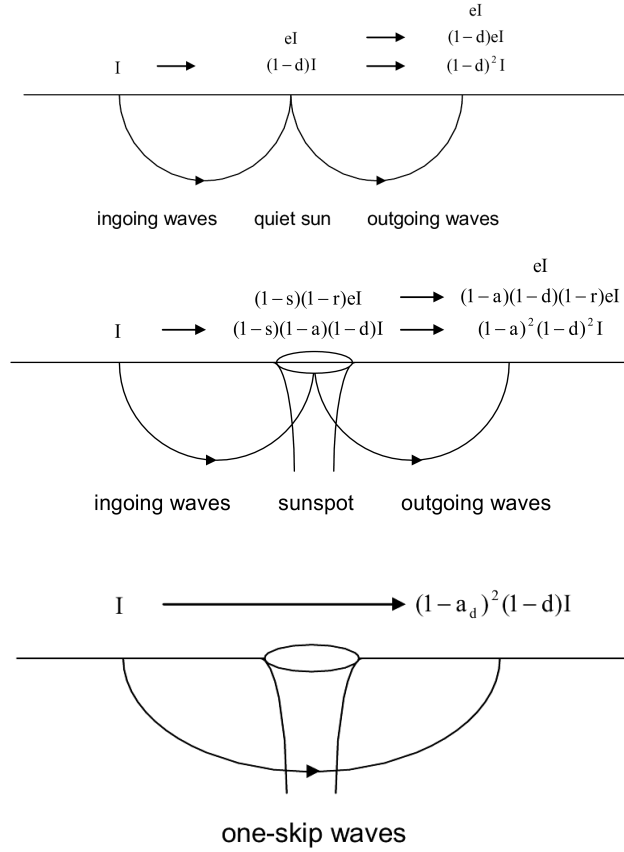


Figure 1. Energy budget of ingoing, outgoing, and double-skip waves propagating through the quiet Sun (top), ingoing, outgoing, and double-skip waves propagating through a sunspot (middle), and one-skip waves propagating through a sunspot (bottom). Only terms connected by arrows correlate.

2. Method

The energy budget of acoustic waves propagating through the quiet Sun and a sunspot is illustrated in Figure 1. The energy of a wave packet associated with a particular travel distance and propagating in a particular direction in the quiet Sun is constant and is denoted here by I . As the waves propagate through the solar medium in the top diagram of Figure 1, the acoustic energy after one skip is reduced by a factor of $(1-d(r))$ due to dissipation, where d is the dissipation coefficient in the quiet Sun and r is the one-skip travel distance. At the same time new waves with energy $e(r)I$ are generated by turbulent convection where $e(r)$ is the emissivity coefficient in the quiet Sun. Since the acoustic energy is constant in the quiet Sun, $e(r) = d(r)$.

For the two signals, $(1-d(r))I$ and $e(r)I$, only the first one correlates with the signal I because $e(r)I$ is generated near the location of reflection by a different

source. We use the above property to determine the dissipation of acoustic waves $d(r)$ in the quiet Sun. If the energy I of the acoustic waves is reduced by a factor of $(1 - d(r))$ after each skip, the energy of the same signal after n skips will be $(1 - d(r))^n I$. Using the definition of cross-covariance between two points as given in Equation (1), we compute the ratio of amplitude of the cross-covariance at the fifth skip, F_5 , to that at the first skip F_1 . Here the wave function Ψ is the square root of the energy. According to Equation (1), $F_5 = (1 - d)^{5/2} I$ and $F_1 = \sqrt{(1 - d)} I$. Equation (2) gives the dissipation in terms of F_5 and F_1 . The exact computational procedure used to determine $d(r)$ is described in the second paragraph of Section 3.

$$F_{12}(\tau) = \sum_t \Psi_1(t) \Psi_2(t + \tau) \quad (1)$$

$$d(r) = 1 - \left(\frac{F_5}{F_1} \right)^{1/2} \quad (2)$$

For the energy budget of the acoustic waves in the sunspot, we follow the model suggested by Chou *et al.* (2009c) but incorporate a minor modification. According to this model the terms $(1 - d(r))I$ and $e(r)I$ that were mentioned before in the quiet Sun are reduced by the factors $(1 - a(r))(1 - s(r))$ and $(1 - s(r))(1 - r(r))$ respectively inside the sunspot, where a is the absorption coefficient, r is the emissivity reduction coefficient, and s is the local suppression coefficient. After one more skip, the acoustic waves propagate outside the sunspot in the region of the quiet Sun. Both terms are further reduced by a factor of $(1 - a(r))(1 - d(r))$ and amplified by a factor of $(1 - s(r))$ because local suppression disappears outside the sunspot. At the location of the second skip, in addition to the terms described above, new waves with energy $e(r)I$ are generated by turbulent convection. For more details of this model see Chou *et al.* (2009c).

We consider now a reference point on the surface of the quiet Sun. Using the definition of cross-covariance as given in Equation (1), we compute the amplitude of cross-covariances of ingoing, outgoing, and two-skip waves with respect to the reference point as functions of travel distance from that point. The two-skip waves have a reflection located in the reference point. The exactly same procedure is applied to the case of a sunspot where the reference point is always inside the sunspot. Considering the ratios of amplitude of the cross-covariance for the ingoing, outgoing and two-skip waves in the sunspot to that in the quiet Sun, we have a closed system of three equations with three variables: absorption, emissivity reduction, and local suppression. By computing ratios of measured values in the sunspots to that in the quiet Sun, we have avoided normalizing our computations, thus making our derivations of those coefficients more accurate. The cross-covariances of ingoing, outgoing, and two-skip waves for the quiet Sun and the sunspot are given in Equations (3)–(8). The solution of the system is given in equations (9)–(11). We should note here that although the waves in Figure 1 are associated with a particular travel distance, the coefficients of absorption, emissivity reduction, and local suppression, as defined in Equations (9)–(11) are functions of the travel distance r . We have

$$F_{\text{out}}^q = \sqrt{1-d}I \quad (3)$$

$$F_{\text{in}}^q = \sqrt{1-d}I \quad (4)$$

$$F_{2\text{skip}}^q = (1-d)I \quad (5)$$

$$F_{\text{in}}^s = \sqrt{(1-s)(1-a)(1-d)}I \quad (6)$$

$$F_{\text{out}}^s = \sqrt{(1-d)(1-a)(1-s)}[(1-a)(1-d) + (1-r)d]I \quad (7)$$

$$F_{2\text{skip}}^s = (1-d)(1-a)I \quad (8)$$

$$a = 1 - \frac{F_{2\text{skip}}^s}{F_{2\text{skip}}^q} \quad (9)$$

$$r = 1 - \frac{1}{d} \cdot \left[\frac{F_{\text{out}}^s}{F_{\text{out}}^q} \frac{F_{\text{in}}^q}{F_{\text{in}}^s} - \frac{F_{2\text{skip}}^s}{F_{2\text{skip}}^q} (1-d) \right] \quad (10)$$

$$s = 1 - \left(\frac{F_{\text{in}}^s}{F_{\text{in}}^q} \right)^2 \frac{F_{2\text{skip}}^q}{F_{2\text{skip}}^s} \quad (11)$$

A similar procedure is followed for one-skip waves. The ray path of these waves is illustrated in the bottom panel of Figure 1. The main difference of the one-skip waves from the two-skip waves is that the one-skip waves encounter the sunspot in deeper layers and do not have upper turning points located inside the magnetized photosphere, thus they can probe the absorption efficiency of the sunspot at these depths. It is natural to define a new absorption coefficient for the one-skip waves as $a_d = 1 - (F_{1\text{skip}}^s/F_{1\text{skip}}^q)^2$. However, using the same definition for the absorption coefficient as the one used for the two-skip waves allows for a direct comparison of the results obtained with these two methods. The absorption as measured by the one-skip waves is called hereafter “deep absorption” to be distinguished from the “surface absorption” measured by the two-skip waves and defined in Equation (9). The “deep absorption” is defined similarly as

$$a_d = 1 - \frac{F_{1\text{skip}}^s}{F_{1\text{skip}}^q} \quad (12)$$

The propagation of acoustic waves in the Sun is affected by dispersion. Dispersion increases the width and hence decreases the amplitude of the cross-covariance. However, if dissipation and absorption are ignored, the product of the square of the amplitude and the width of the cross-covariance is constant (Chou and Ladenkov, 2007; Burtseva *et al.*, 2007). In order to correct the effect of dispersion, the width-corrected cross-covariance \tilde{F}_{ab} is defined as

$$\tilde{F}_{ab} = F_{ab}(w_{ab})^{1/2} \quad (13)$$

where w_{ab} is the ratio of the width of the cross-covariance at point b to that at point a . All of the cross-covariances presented in this paper are width corrected.

3. Data Analysis and Results

Doppler observations from MDI onboard the *Solar and Heliospheric Observatory* (Scherrer *et al.*, 1995) are used in this work. The study of ingoing, outgoing, one- and two-skip waves both for the active regions and the quiet Sun utilizes 31 datasets, selected from 1996 to 2001. Each dataset is 512 minutes long, tracked with a Carrington rotation rate and remapped to Postel's coordinates centered at the main active region, with a spatial resolution of $0.12^\circ \text{ pixel}^{-1}$ and a size of 256×256 pixels. Each dataset is then filtered in the Fourier domain to remove solar convection and f modes. We do not filter out signals above the cut-off frequency since most of acoustic power is concentrated below the cut-off limit and our experiments also show that with and without filtering those signals, our results do not change.

The computational procedure starts with the determination of dissipation in the quiet Sun that appears in Equation (10). We select 900 pixels from each dataset to compute center-to-annulus cross-covariances with the time–distance helioseismology technique (Duvall *et al.*, 1993; Kosovichev, Duvall, and Scherrer, 2000). Two concentric quadrants are selected around a central pixel so that the radius of the larger quadrant is five times larger than that of the smaller one. The signal inside the quadrants is averaged, and the cross-covariance between the signal of the central pixel and the averaged signal of each quadrant is computed for both positive and negative travel-time lags. Each cross-covariance is then multiplied by the length of the corresponding quadrant because, in the absence of a direction filter, the acoustic energy, propagating from the central pixel to the quadrant, is uniformly distributed over it. The same procedure is repeated for a range of radii of 11 – 45 pixels and all of the cross-covariances for the same distances and for both time lags, obtained from different central pixels and different datasets, are combined to increase the signal-to-noise ratio. For larger travel distances of 46 – 54 pixels, the use of five skips is not possible due to the limited size of the dataset and thus only four skips were used. Equation (2) is modified for this case to $d(r) = 1 - (F_4/F_1)^{2/3}$. The one- and the five-skip (or four-skip) signals are fitted with a Gabor wavelet function (Kosovichev and Duvall, 1996) and the amplitudes and widths of the two cross-covariances are obtained. The dissipation is calculated using Equations (2) and (13) and the result is presented in Figure 2.

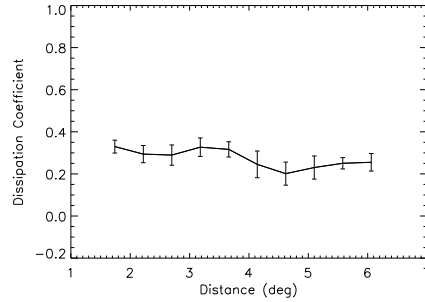


Figure 2. Dissipation coefficient in the quiet Sun as a function of acoustic wave-travel distance.

We should point out that an accurate measurement of dissipation is crucial for the work that follows since the dissipation coefficient appears in Equation (10) that is used to determine the emissivity reduction. The approach followed here is based on measurements of an amplitude ratio of five-skip (or four-skip) signals to one-skip signals. In fact any number of skips can be used to determine the dissipation coefficient. Therefore, the ratio of five-skip signal-to-one-skip signal in Equation (2) can be a ratio of two skips to one skip or three skips to two skips *etc.* Since after each skip the acoustic energy is reduced by a factor of $(1 - d(r))$, the larger the difference of skips in the ratio of Equation (2), the larger the dissipated energy. So using more skips makes our measurements more accurate. The use of more than five-skip signals is not possible due to the limited size of the dataset, so for the dissipation coefficient presented in Figure 2, five skips are used for distances up to 5.4° and four skips for larger distances. The two methods, as well as others with different combinations of skips, are consistent with the only difference being that the signal-to-noise ratio is higher for those methods where the dissipated energy is larger.

Next we determine the absorption, emissivity reduction, and local suppression coefficients inside active regions. This study includes 47 active regions distributed in 31 datasets. The strength of the magnetic field in the magnetograms, which were obtained at the same time with same resolution as the Dopplergrams, is used as the criterion to select the pixels inside the active region in the corresponding Dopplergrams. Setting the threshold at 1100 G and 500 G, we select approximately the pixels inside the umbra and both the umbra and penumbra (sunspot) respectively. Each one of these pixels is used to compute center-to-annulus cross-covariances. An annulus around the central pixel is selected and the signal inside this annulus is averaged. The cross-covariance between the central pixel and the averaged signal inside the annulus is computed for both positive and negative travel-time lags. The positive travel-time lag corresponds to outgoing waves and the negative travel-time lag corresponds to ingoing waves. The same procedure is repeated for a range of radii of 11 – 54 pixels and all of the cross-covariances for the same distances, obtained from different central pixels and different datasets, are combined to increase the signal-to-noise ratio. The signals corresponding to outgoing and ingoing waves are fitted with a Gabor wavelet function and the amplitudes and widths of the two signals are obtained.

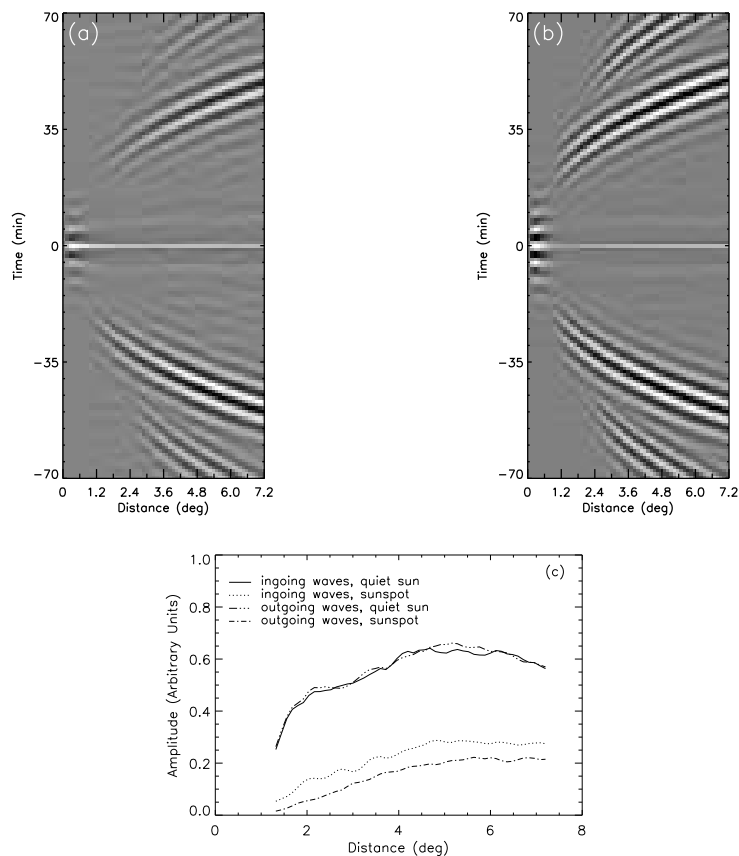


Figure 3. Time–distance diagrams of ingoing and outgoing waves for (a) sunspots and (b) quiet Sun. The positive travel–time lag corresponds to outgoing waves and the negative to ingoing waves. The amplitude fittings of the cross-covariance function are shown in panel (c).

For the one- and two-skip waves, the annulus around the central pixel is divided into four quadrants and the signal inside each one of them is averaged. The cross-covariance is computed between the two pairs of diametrically opposite quadrants for both positive and negative travel-time lags. The process is repeated again for the same range of radii and all the cross-covariances for the same distances and for both time lags, obtained from different central pixels and different datasets, are combined. The two-skip signal is again fitted with a Gabor wavelet function and the amplitude and width of the signal are obtained. The exactly same procedures are carried out for the quiet Sun to obtain cross-covariances as references. The time–distance diagrams for the sunspot and the quiet Sun as well as the amplitude fittings of the ingoing and outgoing waves are shown in Figure 3. The corresponding time–distance diagrams and amplitude fittings for the one- and two-skip waves are shown in Figure 4. The three coefficients of absorption, emissivity reduction, and local suppression are computed using Equations (9)–(11) and the results are presented in Figures 5 and 6. The error

bar corresponds to the standard deviation of those measurements from which mean values are obtained.

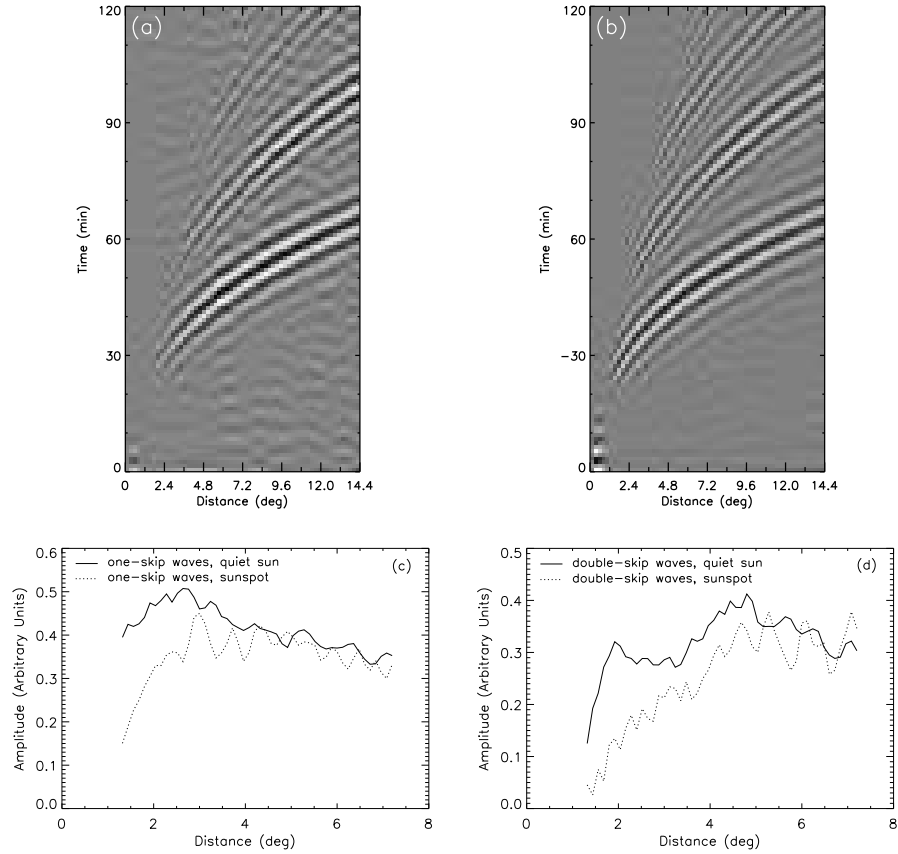


Figure 4. Time–distance diagrams of one- and two-skip measurements for (a) sunspots and (b) quiet Sun. Amplitude fitting of the cross-covariance function for (c) one-skip waves and (d) two-skip waves.

In the model of Figure 1, the beginning point is assumed to have the power of the quiet Sun. If that is not the case, an error will arise in the computation of the cross-covariances and the coefficients of absorption, emissivity reduction, and local suppression (Chou *et al.*, 2009d). In order to make our measurements as accurate as possible, the computation of cross-covariances includes only those pixels for which the magnetic field at the beginning point of Figure 1 is lower than an arbitrary threshold, which is set to 40 G. For the selection of pixels in the quiet Sun, the closest magnetic region to the quiet pixel is at least nine pixels away from it. The magnetic region is defined as a region where the magnetic field is higher than 500 G. For some large active regions, the annuli of short distances are located completely inside the sunspot and thus no pixel from those annuli can be used for the computation of center-to-annulus cross-covariances. In this case we use the average cross-covariance with same annulus distance from the

central pixel, as calculated from all other central pixels of the same dataset. The algorithm described above makes sure that the computation of cross-covariances for the sunspot and the quiet Sun uses the exactly same number of annuli. However, it is possible that at short distances a significant number of pixels in the annuli are excluded from the computation of cross-covariances and therefore the accuracy of the measurements can be affected.

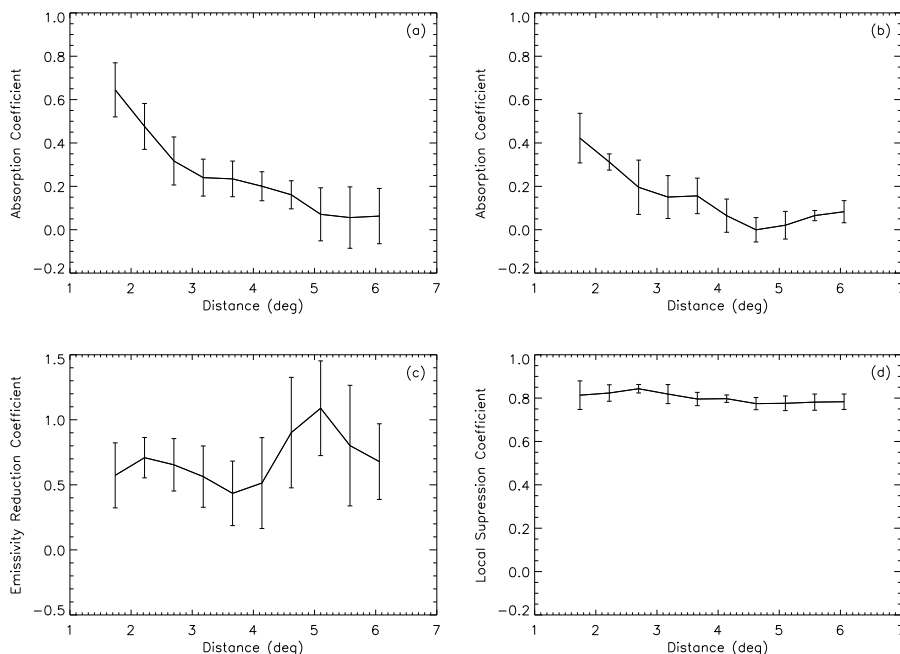


Figure 5. Coefficients of (a) surface absorption, (b) deep absorption, (c) emissivity reduction, and (d) local suppression obtained from umbral measurements (threshold of 1100 G).

The measurements of ingoing and outgoing waves are less noisy than those of one- and two-skip waves. This can be seen either from the time–distance diagrams in Figures 3 and 4 or from the amplitude fittings of those diagrams. However, in both cases the amplitude and width of the cross-covariance function can easily be obtained by our method. For the quiet Sun, ingoing and outgoing waves have approximately equal amplitudes. On the contrary, for sunspot measurements the amplitude of outgoing waves is reduced compared to that of ingoing waves. The one- and two-skip wave amplitudes show a different trend. At short travel distances, the wave amplitude in the quiet Sun is much greater than that in sunspot but at large travel distances the two amplitudes are comparable within the noise level of the measurements.

The surface absorption coefficient, presented in Figures 5a and 6a, is a maximum at the shortest travel distances and smoothly drops to zero at distance of about 6°. This picture is consistent with previous work (for example Braun, Duvall, and LaBonte, 1987, 1988; Bogdan *et al.*, 1993; Chen *et al.*, 1996). However, a quantitative comparison is not possible, first due to the different definitions of

absorption and second because our definition separates the effects of absorption and emissivity reduction. The deep absorption follows the same trend but compared to the surface absorption is about 40% smaller at small travel distances where both of them are greater than zero. At large travel distances they both drop to zero and become comparable. The emissivity reduction coefficient is most noisy due to the several terms involved in Equation (10). Inside umbrae emissivity reduction is rather high ranging from 0.44 to 1.00 with a mean value of 0.70, while in the whole sunspot the corresponding range is 0.29 to 0.72 averaging 0.47. The local suppression coefficient is very constant within the range of travel distances used in this work. Its mean values for umbral and penumbral measurements are 0.80 and 0.665 respectively.

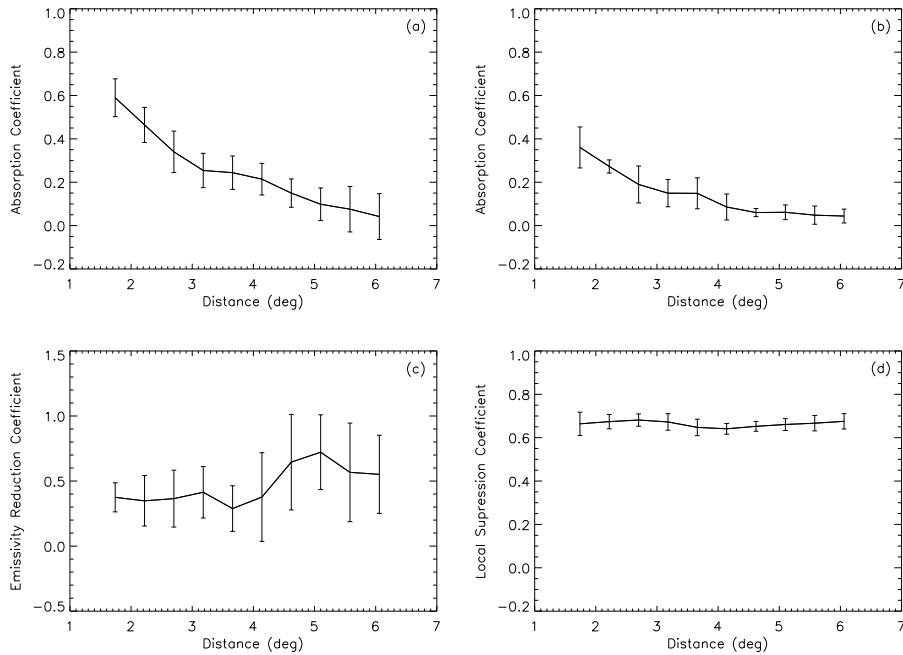


Figure 6. Coefficients of (a) surface absorption, (b) deep absorption, (c) emissivity reduction, and (d) local suppression obtained from sunspot measurements (threshold of 500 G).

All three coefficients of absorption, emissivity reduction, and local suppression, as defined in this work, contribute to the power deficit inside sunspots. However, it is not clear, from this definition, what is the exact contribution of each coefficient to the total power deficit in sunspots. It is more appropriate to define three normalized coefficients so that each is equal to the fraction of the contribution of the corresponding mechanism to the total power deficit inside the sunspot. According to the energy budget of the acoustic waves in the sunspot, the normalized coefficients are

$$a_* = \frac{a(1-d)}{1-P} \quad (14)$$

$$r_* = \frac{rd}{1-P} \quad (15)$$

$$s_* = \frac{s[(1-a)(1-d) + (1-r)d]}{1-P} \quad (16)$$

where $P = (1-s)(1-a)(1-d) + (1-s)(1-r)d$ is the total acoustic power inside the sunspot. It is easily shown that $a_* + r_* + s_* = 1$. The normalized coefficients are plotted as functions of travel distance in Figure 7.

The definition of normalized coefficients allows a direct comparison of the results obtained in this work with results from previous works. Chou *et al.* (2009c), using the same definition, found that the fractional contribution of each mechanism to the acoustic power deficit in the umbra of the sunspot for a specific wave packet that corresponds to travel distance of 3.5° is $a = 0.233$, $s = 0.685$ and $r = 0.082$. For the same travel distance, we found $a = 0.187$, $s = 0.652$ and $r = 0.161$. The two methods are consistent in local suppression but not in absorption and emissivity reduction. The absorption in Chou *et al.* is larger compared to our work while the emissivity reduction is smaller. However, the results obtained in this work are based on averaged measurements over 46 sunspots while the results presented by Chou *et al.* are based on a single sunspot. Not only are the two samples different but it is also possible that there are significant variations among the 47 sunspots analyzed in this study. Especially the coefficients of absorption and emissivity reduction may have strong dependence on the size of the sunspot and the strength of the magnetic field. It would be interesting to use the sample of 47 sunspots to study this dependence. Our method does not make use of phase-speed and direction filters though, and consequently, time-distance measurements with individual sunspots are very hard, if not impossible. In practice, the low number of total pixels increases the noise level in the cross-covariance function for the one- and especially for the two-skip waves, making the measurement of the amplitude very hard.

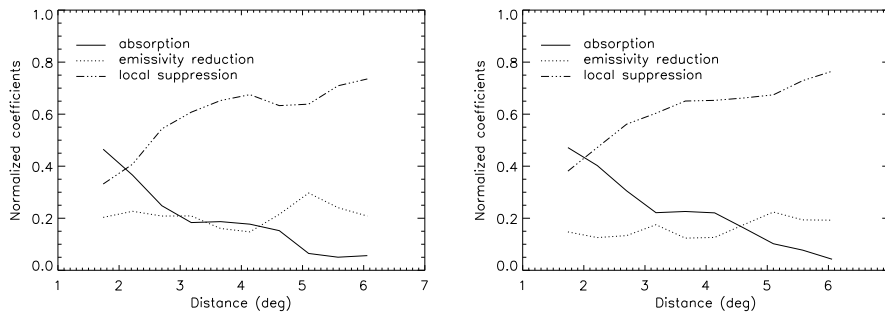


Figure 7. Normalized coefficients as functions of the travel distance for the umbral measurements (left) and the sunspot measurements (right).

4. Summary

We apply a new method to measure the coefficients of absorption, emissivity reduction, and local suppression inside solar active regions as well as the coefficient of dissipation in the quiet Sun. This method utilizes measurements from many active regions to increase the signal-to-noise ratio, and does not use signal filters except filtering out solar convection and f -modes. All four coefficients are determined as functions of the travel distance. Comparison with previous work for a specific travel distance shows good agreement in the coefficient of local suppression but discrepancies in coefficients of absorption and emissivity reduction. It is not clear though if these discrepancies are caused by the different method used in each case or by the different samples of sunspots. In summary, our results show the following:

- i The absorption coefficient is the dominant mechanism for the power deficit in sunspots at short distances but it gradually drops to zero at travel distance of about 6° .
- ii The measured deep absorption is about 60% as high as the measured surface absorption indicating that sunspots can actually absorb a large amount of acoustic energy not only close to the surface but also deep below the photosphere.
- iii The emissivity reduction coefficient ranges between 0.44 and 1.00 within the umbra with a mean value of 0.70, and between 0.29 and 0.72 within the sunspot with a mean value of 0.47. The fractional contribution to the acoustic power deficit in sunspots is 21.5% for the umbra and 16.5% for the sunspot.
- iv The local suppression coefficient is remarkably constant as a function of the travel distance with a value of 0.80 for the umbral measurements and 0.665 for the sunspot measurements. Its fractional contribution to the acoustic power deficit increases smoothly as a function of the travel distance from 33% to 75% in the umbra and from 38% to 79% in the sunspot.

References

- Bogdan, T., Brown, T., Lites, B., Thomas, J.: 1993, *Astrophys. J.* **406**, 723.
 Braun, D.C., Duvall, T.L. Jr., LaBonte, B.J.: 1987, *Astrophys. J. Lett.* **319**, L27.
 Braun, D.C., Duvall, T.L. Jr., LaBonte, B.J.: 1988, *Astrophys. J.* **335**, 1015.
 Burtseva, O., Kholikov, S., Serebryanskiy, A., Chou, D.-Y.: 2007, *Solar Phys.* **241**, 17.
 Cally, P.S., Bogdan, T.J.: 1993, *Astrophys. J.* **402**, 721.
 Cally, P.S., Bogdan, T.J., Zweibel, E.G.: 1994, *Astrophys. J.* **437**, 505.
 Chen, K.-R., Chou, D.-Y., and the TON team: 1996, *Astrophys. J.* **465**, 985.
 Chou, D.-Y., Ladenkov, O.: 2007, *Solar Phys.* **241**, 7.
 Chou, D.-Y., Liang, Z.-C., Yang, M.-H., Sun, M.-T.: 2009a, *Solar Phys.* **255**, 39.
 Chou, D.-Y., Yang, M.-H., Liang, Z.-C., Sun, M.-T.: 2009b, *Astrophys. J. Lett.* **690**, L23.
 Chou, D.-Y., Liang, Z.-C., Yang, M.-H., Zhao, H., Sun, M.-T.: 2009c, *Astrophys. J. Lett.* **696**, L106.
 Chou, D.-Y., Yang, M.-H., Zhao, H., Liang, Z.-C., Sun, M.-T.: 2009d, *Astrophys. J.* **706**, 909.
 Crouch, A.D., Cally, P.S.: 2005, *Solar Phys.* **227**, 1.

- Duvall, T.L. Jr., Jefferies, S.M., Harvey, J.W., Pomerantz, M.A.: 1993, *Nature* **362**, 430.
- Goossens, M., Poedts, S.: 1992, *Astrophys. J.* **384**, 348.
- Gordovskyy, M., Jain, R.: 2008, *Astrophys. J.* **681**, 664.
- Hindman, B.W., Jain, R., Zweibel, E.G.: 1997, *Astrophys. J.* **476**, 392.
- Hollweg, J.: 1988, *Astrophys. J.* **335**, 1005.
- Hurlburt, N., Toomre, J.: 1988, *Astrophys. J.* **327**, 920.
- Kosovichev, A.G., Duvall, T.L. Jr.: 1996, In: Pijpers, F.P., Christensen-Dalsgaard, J., Rosenthal, C.S. (eds.) *Proc. SCORe'96 Workshop: Solar Convection and Oscillations and Their Relationship*, Kluwer, Dordrecht, 241.
- Kosovichev, A.G., Duvall, T.L. Jr., Scherrer, P.H.: 2000, *Solar Phys.* **192**, 159.
- Leighton, R., Noyes, R., Simon, G.: 1962, *Astrophys. J.* **135**, 474.
- Lites, B.W., White, O.R., Packman, D.: 1982, *Astrophys. J.* **253**, 386.
- Lou, Y.-Q.: 1990, *Astrophys. J.* **350**, 452.
- Parchevsky, K.V., Kosovichev, A.G.: 2007, *Astrophys. J. Lett.* **666**, L53.
- Rajaguru, S.P., Sankarasubramanian, K., Wachter, R., Scherrer, P.H.: 2007, *Astrophys. J. Lett.* **654**, L178.
- Sakurai, T., Goossens, M., Hollweg, J.V.: 1991, *Solar Phys.* **133**, 247.
- Scherrer, P.H., Bogart, R.S., Bush, R.I., Hoeksema, J.T., Kosovichev, A.G., Schou, J., Rosenberg, W., Springer, L., Tarbell, T.D., Title, A., *et al.*: 1995, *Solar Phys.* **162**, 129.
- Spruit, H.C., Bogdan, T.J.: 1992, *Astrophys. J. Lett.* **391**, L109.
- Wachter, R., Schou, J., Sankarasubramanian, K.: 2006, *Astrophys. J.* **648**, 1256.